Title

Synthesis and optimization of collagen-targeting peptide-glycosaminoglycans for inhibition of platelets following endothelial injury

Journal

Proteoglycan Research, 1(2)

ISSN

2832-3556

Authors

Nguyen, Michael

Walimbe, Tanaya

Woolley, Andrew

et al.

Publication Date

2023-04-01

DOI

10.1002/pgr2.3

Peer reviewed

HHS Public Access

Author manuscript

Proteoglycan Res. Author manuscript; available in PMC 2024 June 14.

Published in final edited form as:

Proteoglycan Res. 2023 April 01; 1(2): . doi:10.1002/pgr2.3.

Synthesis and Optimization of Collagen-targeting Peptide-Glycosaminoglycans for Inhibition of Platelets Following Endothelial Injury

Michael Nguyen[a], **Tanaya Walimbe**[a,b], **Andrew Woolley**[b], **John Paderi**[b], **Alyssa Panitch**[a,c,*]

[a]Department of Biomedical Engineering, University of California, Davis, USA

[b]Symic Bio, USA

[c]Wallace H. Coulter Department of Biomedical Engineering, Georgia Institute of Technology and Emory University, USA

Abstract

Many endothelial complications, whether from surgical or pathological origins, can result in the denudation of the endothelial layer and the exposure of collagen. Exposure of collagen results in the activation of platelets, leading to thrombotic and inflammatory cascades that ultimately result in vessel stenosis. We have previously reported the use of peptide-GAG compounds to target exposed collagen following endothelial injury. In this paper we optimize the spacer sequence of our collagen binding peptide to increase its conjugation to GAG backbones and increase the peptide-GAG collagen binding affinity by increasing peptide C-terminal cationic charge. Furthermore, we demonstrate the use of these molecules to inhibit platelet activation through collagen blocking, as well as their localization to exposed vascular collagen following systemic delivery. Altogether, optimization of peptide sequence and linkage chemistry can allow for increased conjugation and function, having implications for glycoconjugate use in other clinical applications.

Keywords

Glycosaminoglycan; peptide; collagen; platelet

INTRODUCTION:

Glycosaminoglycans (GAGs) represent a century-old drug class of carbohydrates with wide therapeutic potential. Numerous clinical and preclinical studies have demonstrated

*Corresponding Author alyssa.panitch@bme.gatech.edu; alyssa.panitch@emory.edu.

Conflict of Interest Statement: JP and AP both own <2 % of Symic Holdings. Symic Holdings owns patent rights to glycosaminoglycans conjugated to collagen binding peptides.

Supporting Information:

- MALDI-TOF MS spectra of CS + SRR-hyd, CS + SRR-SRR-amide, and CS+GSG-hyd before salt and urea wash; MALDI-TOF MS spectra of CS + SRR-hyd, CS + SRR-SRR-amide, and CS+GSG-hyd after salt and urea wash; MALDI-TOF MS spectra of CS + SRR-hyd and Hep + SRR-hyd before salt and urea wash; MALDI-TOF MS spectra of CS + SRR-hyd and Hep + SRR-hyd after salt and urea wash

the efficacy of GAGs in a broad range of diseases, including cancers, cardiovascular disease, fibrosis, and autoimmune disorders (J. Paderi et al., 2018; Wang et al., 2022). One of the recognized challenges of GAGs is their suboptimal pharmacokinetic profile when administered parenterally, thus limiting their use more broadly(Malloy et al., 2018). Targeted drug delivery strategies can overcome this limitation, providing for a robust approach to generate innovative new GAG therapeutics (J. Paderi et al., 2018; Strobel et al., 2018).

We have identified collagen as a key therapeutic target as collagens are frequently exposed in disease states or during injurious surgical or endovascular procedures. Exposure of collagen to blood triggers a potent platelet activation response and subsequent thrombotic and inflammatory processes (Manon-Jensen et al., 2016; Nording et al., 2015). During endovascular procedures or in vascular surgeries, for example, the fragile endothelial layer is often denuded, and the platelet-mediated inflammatory response contributes to an adverse hyperplastic healing sequalae that causes vessel stenosis. Endothelial dysfunction can lead to collagen exposure in numerous disease states such as in cancer, autoimmune disorders such as systemic sclerosis (Harifi & Sibilia, 2016), infectious diseases including COVID-19 (D'Agnillo et al., 2021), and in fibrosis (Karsdal et al., 2017). Collagen is therefore a prime target, as it is both a target for delivery to specific areas of injury or disease, and is also itself a contributing pathomechanism for adverse healing and disease progression.

We have previously designed collagen-binding peptide-modified GAGs as therapeutics that target endothelial injury and inhibit platelet activation in the lumen of a blood vessel when delivered locally (J. E. Paderi et al., 2011; Scott et al., 2013). Systemic delivery of these compounds is limited, however, due to the relatively low affinity of these compounds. We have therefore aimed to improve the binding affinity of these compounds to enable systemic administration with targeted delivery to areas of exposed collagen, as occurs in injury or disease. Generally, optimization strategies include peptide binding affinity, linkage chemistry, spacer optimization between the GAG and the binding domain of the peptide, and conservation of the GAG's therapeutic activity.

Glycosaminoglycans are negatively charged linear carbohydrate chains and include sulfated GAGs such as heparin (Hep), dermatan sulfate (DS), and chondroitin sulfate (CS), or non-sulfated carbohydrates including hyaluronan (HA) (Vallet et al., 2021). Given the broad therapeutic activity of GAGs and their biocompatibility, multiple chemical strategies have been employed for modifying GAGs including adding payload(Han et al., 2006), immobilizing to surfaces such as vascular grafts(Biran & Pond, 2017), generating scaffolds or hydrogels (Liang & Kiick, 2014), or creating micro- or nano-particle therapeutic agents (Das Kurmi et al., 2015). The negative charge and charge density of GAGs is important for biological activity and the interaction of GAGs with numerous biological binding partners (Capila & Linhardt, 2002). The negative charge also influences modification and purification strategies of GAGs, where charged groups can associate(Schick et al., 2004), lead to precipitation (Cho & Han Ahn, 2013), or mask binding regions.

In unpublished studies we identified a modified version of the collagen-binding peptide identified by Chiang and Kang that also binding to collagen, but does not contain thiol or carboxylate groups (GQLYKSILY) (Chiang & Kang, 1997). Furthermore, we have

previously reported that there is a balance between GAG modification and preservation of GAG activity (Nguyen et al., 2021). Others have shown that GAG oxidation affect GAG activity; specifically, heparin oxidation reduces the anticoagulation activity of heparin without affecting its susceptibility to heparinase activity (Naggi et al., 2005). Thus, we focus our efforts on modification through the carboxylate groups on the GAG using peptide-hydrazides, as hydrazides are more reactive under acidic condition than are amines that are present at the N-terminus and on lysine residues present within the peptide. As depicted in Figure 1, here we investigated whether inclusion of cationic charge within the spacer region and proximal to hydrazide group would improve peptide-GAG conjugation as a step toward optimizing collagen-binding potency of the peptide-GAG for targeted delivery to areas of vascular injury or disease while also preserving the GAG antiplatelet function.

Materials and Methods:

2.1: Synthesis of GQLY Peptide Variants

The purified peptide SSR-hyd (GQLYKSILYGSGSGSRR-hyd) was purchased from Chinese Peptide Company. GQLY variants SRR-amide (GQLYKSILYGSGSGSRR-amide) and GSG-hyd (GQLYKSILYGSGSG-hyd) were synthesized using solid phase peptide synthesis chemistry, on Rink Amide resin (CEM Corporation) or hydrazide loaded Cl-TCP(Cl) resin (CEM Corporation) to functionalize the peptide C terminus with an amide or hydrazide group, respectively. Peptide synthesis was performed using a Liberty Blue peptide synthesizer, with post synthesis cleavage of the peptide from the resin being carried out using a cocktail of trifluoracetic acid, triisopropylsilane, phenol, and water. Peptides were purified using fast protein liquid chromatography (FPLC), with the peptide molecular weight in the collected fractions verified using matrix assisted laser desorption/ionization time of flight mass spectrometry (MALDI-TOF MS). Peptides were then frozen, lyophilized, and stored at −80 °C until later use.

2.2: Synthesis and Analysis of GAG-GQLY Variants

The GAGs heparin (average M_W = 12.5 kDa, purity = >90% Bioiberica), hyaluronic acid (average M_W = 60 kDa, purity = >95% Lifecore Biomedical), chondroitin sulfate (average M_W = 40 kDa, purity = >98%, Seikigaku Corporation), and dermatan sulfate (average M_W = 35 kDa, purity = >90%, Bioiberica) were reacted with GQLY peptide variants using aqueous carbodiimide chemistry. GAGs were dissolved in a solution of 0.1 M 2-(N-morpholino)ethanesulfonic acid (MES), 8M urea, and 0.2 wt% sodium chloride at a concentration of 10 mg/mL. Solid peptide was dissolved in the solution to theoretically functionalize 16% of the GAG disaccharide units present. 1-Ethyl-3-[3-dimethylaminopropyl]carbodiimide (EDC) was then added in a ratio of 0.5:1 EDC to GAG disaccharide units, where number of disaccharide units were determined by dividing the total mass of GAG by the mass of one disaccharide unit. The reaction was titrated to pH 4.5 and allowed to proceed overnight. Fluorescently labeled compounds were synthesized by reacting a 1:1 molar ratio of fluorophore CF-633-hydrazide (Biotium) to GAG followed by peptide conjugation. To purify the solution, the reaction was first titrated to pH 8.5 to stop the reaction, then purified using a KrosFlo tangential flow filtration system. The reactions were purified against a 10 kDa cutoff membrane at a transmembrane pressure of 25 psi

until a permeate volume of 5X the reaction volume had been reached. Solutions were then frozen and lyophilized until further use. Quantification of peptides associated with the GAGs was done by analyzing the ultraviolet absorbance of the purified molecules at 280 nm and calculating the peptide content using standard curves for the respective peptide.

2.3: Structural Analysis of GQLY Variants by Circular Dichroism

The structure of the GQLY variants SRR-hyd and GSG-hyd was analyzed using a Jasco J-715 Circular Dichroism (CD) spectrometer. Samples were dissolved at a concentration of 1 mg/mL in pH 8.5 sodium borate buffer and loaded into a quartz cell. The far-UV spectra of the peptides was measured from 190 to 250 nm, with the structure of the peptides determined from the spectra using BESTSEL (https://bestsel.elte.hu/index.php) (Micsonai et al., 2018). The analysis method calculates individual secondary structural elements using the least-squares method applied at every wavelength point. It also accounts for the twisting angle range of antiparallel β-sheets to differentiate them from other structures and distinguishes regular a α-helix from a distorted α-helix to improve analysis. For a detailed explanation, please read the published work by Micsonai, et al (Micsonai et al., 2015).

2.3: Analysis of CS-GQLY Conjugate Association

To test for the presence of peptides associated with CS through non-covalent interactions, CS reacted with GQLY variants were dissolved in ultrapure water, then analyzed for free peptide using MALDI-TOF MS. To remove any peptide associate with GAGs via non-covalent interactions, CS-GQLY variants were dissolved in a solution of 1 M sodium chloride and 8 M urea to disrupt electrostatic interactions between CS and the GQLY variants. Solutions were agitated for 30 minutes, with any disassociated peptide filtered out using Amicon Ultra centrifugal filter units (Millipore) with a 10 kDa molecular weight cut off filter. Following treatment with the salt solution, the salt concentration of the retentate was diluted by replenishing the volume lost with deionized water, then spin filtering three times. The UV absorbance at 280 nm was of the solutions was taken before and after the disassociation process to quantify the amount of peptide removed from the GAG backbone. Dissociation of electrostatically bound peptide was confirmed using MALDI (Supplementary figure S1–S4)

2.4: Binding Capability of CS-GQLY and Hep-GQLY Variants

To determine how the C-terminal spacer sequence or GAG backbone affected peptide-GAG binding ability, CS-GQLY and Hep-GQLY variants were biotinylated through reacting with EZ-Link Hydrazide-Biotin (ThermoFisher Scientific) using the same EDC carbodiimide synthesis and purification process. For collagen binding capability, a Biocoat collagen type I coated plate (Corning) was first blocked with 5% bovine serum albumin for one hour, then washed three times with phosphate buffered saline (PBS). A logarithmic serial dilution of each CS-GQLY and Hep-GQLY variant in PBS was pipetted onto the plate and was incubated at 37 °C for 30 minutes. The plate was again washed three times with PBS. Next, a 200X dilution solution of streptavidin-horseradish peroxidase solution (R&D Systems) was added and incubated for 20 minutes. Color was developed with a corresponding substrate solution (R&D Systems) for 20 minutes, with reaction stopped with 2N sulfuric acid. The amount of bound molecule was determined through measuring absorbance at 450

nm, with binding curves constructed using GraphPad Prism. The collagen binding EC_{50} for each molecule was determined by fitting the data to a non-linear one-site binding equation Y = Bmax*X/(Kd + X), where the EC_{50} was determined from 50% of the maximum binding capacity for each molecule. For analysis number of disaccharide units were determined by dividing the total mass of GAG by the mass of one disaccharide unit

2.5 Platelet-collagen inhibition studies

Flow channel slides (Ibidi μ-Slide VI 0.1) were coated with 100 μg/mL of Chrono-Par fibrillar collagen type I for 1 h at room temperature. Channels were flushed three times with 1X PBS pH 7.4 (PBS) to remove any unbound collagen. After washing away excess collagen, slides were incubated with Hep-GQLY, unmodified heparin, and unconjugated GQLY at increasing concentrations for 1 h, then flushed three times with 1X PBS to remove unbound peptide-GAG. Following an approved IRB protocol (WIRB protocol # 20,162,858), human blood was collected into citrated vacutainers and was used within 3 h of collection. Whole blood was removed from the vacutainers, pooled and then stained with Calcein-AM at 1 mg/mL in dimethyl sulfoxide (DMSO) for 30 min at 37 °C. Hep-GQLY-SRR was then added to pre-stained human whole blood at various concentrations. Next, blood was perfused across each channel at a physiological shear rate of 1000 s− 1. Adherent cells were imaged using EVOS Fluorescence microscope (ThermoFisher Scientific). Platelet adhesion was quantified using NIH ImageJ software. IC_{50} of treatment molecules was determined by normalizing platelet adhesion to the untreated control, then constructing an inhibition curve by plotting the percent inhibition against the concentration of Hep-GQLY using the model Y= minimun + (maximum-minimum)/(1+10^(X-Log(IC_{50}))) in GraphPad Prism.

2.6 Targeted delivery to injured vessels in vivo

In order to verify, visually, that the GAG-therapeutic targeted exposed collagen within a denuded artery, an arterial crush injury model was used. The arterial crush injury is an efficient model to mimic the endothelial denudation that occurs due to balloon angioplasty, but does not require expensive balloon catheters (Yu et al., 2017). In vivo studies complied with the National Research Council's Guide for the Care and Use of Laboratory Animals. Because collagen is largely conserved across sexes and species, sex as a variable is not expected to impact the results. A rabbit artery crush model was used to investigate the ability of compounds to selectively bind to regions of injury. Female New Zealand rabbits (n=3/group) were anesthetized and the carotid artery was exposed. Blood flow to an artery segment approximately 2 cm was arrested using a non-injurious clamp and blood was subsequently evacuated. Several crush injuries were then created by external clamping for 10 s using a hemostat. Compounds (Either saline control or GAG therapeutic) were then administered in a blinded fashion by ear vein through an IV catheter (1 mL/kg) and blood flow was restored for 2 h. Animals were then euthanized and the arteries were harvested, dissected longitudinally, pinned open to black foam board and fixed with formaldehyde for 1 h before transferring to 1X PBS pH 7.4 and stored at 4° C. The open face of the whole-mount arteries were positioned in a glass coverslip bottom dish (Ibidi μ-Dish) containing PBS and imaged on a LSM710 confocal microscope (Zeiss). Tissue autofluorescence and CF-633-labeled compound were imaged using 488 and 633 lasers, respectively. Maximum-

intensity projections of the 3D-tiled confocal data were analyzed qualitatively by a blinded observer for targeted binding of the fluorescently tagged molecule.

2.7 Statistical Analysis

Data are represented as the mean value of replicates, with error bars corresponding to their standard deviation. For the comparison between two groups, statistical significance was determined using a T-Test. For comparisons between three or more groups, a single factor equal variance ANOVA was performed. Differences between specific groups was determined using Tukey's post hoc test. Statistical analysis was performed using Graphpad Prism, with a probability value of 95% ($P < 0.05$) being used to determined statistical significance.

Results and Discussion:

3.1: Effect of SRR Spacer on GQLY Conjugation and Collagen Binding Activity

Peptide conjugation, peptide-GAG interaction, and collagen experiments were initially carried out with CS due to the intermediate degree of sulfation and molecular weight of CS relative to other GAGs studied. To investigate the effects of C-terminal cationic charge on molecule synthesis and collagen-binding activity, two variants of the GQLY peptide were synthesized, one with a C-terminal spacer sequence of GSGSG, GQLYKSILYGSGSG-hydrazide (GSG-hyd), and one with C-terminal spacer sequence of GSGSRR, GQLYKSILYGSGSGSRR-hydrazide (SRR-hyd). CD analysis of both variants showed minimal difference in their structure, indicating that the addition of the SRR spacer did not significantly alter the structure of GQLY (Figure 2, Table 1). Given the negative charge of the GAG backbone, it was theorized that the addition of positive charges conferred by the arginine residues proximal to C terminus would influence the peptide's association with the sulfated GAG backbone. Following the peptide – GAG reaction in which EDC was used to activate the GAG carbonyl-groups, there was significantly more peptide association when using the SRR-hyd variant compared to the GSG-hyd variant (Figure 2). This suggested that the additional positive charge present in the SRR spacer increased the GQLY peptide interaction with the negatively charged CS backbone.

While increased SRR-hyd peptide was found associated with the GAG, the method of peptide detection could not differentiate between covalently bound peptide and electrostatically bound peptide. To determine whether peptide remained bound electrostatically even following initial purification against a 10 kDa membrane, the peptide-GAGs were synthesized in the absence of EDC to eliminate covalent bonds formation between peptide and GAG. Again, significantly more of the SRR-hyd variant associated with CS compared to the GSG-hyd variant following the initial purification showing that the cationic SRR spacer was driving electrostatic interactions (Figure 3a). To probe the difference in covalent and electrostatic association, peptide-GAG was reacted with EDC then washed with a concentrated salt and urea solution to disrupt the electrostatic interactions, with the liberated peptide removed through centrifugation against a 10 kDa cutoff membrane. By measuring the associated peptide before and after this second purification, the amount of covalently bound peptide could be determined. Following salt

washes, there was a 32% decrease in total amount of SRR-hyd associated peptides with a corresponding decrease of 5.1% in peptides associated per disaccharide, whereas there was only a 15% decrease in the total amount of GSG-hyd associated peptides with a corresponding decrease of 1.1% in peptides associated per disaccharide (Figure 3b, Table 2). Furthermore, the SRR-hyd group still exhibited increased association with CS compared the GSG-hyd group, suggesting that the SRR spacer sequence also had a positive effect on covalent conjugation. Similar trends were seen when measuring the zeta potentials of the peptide-GAGs before and after disassociation, where the molecules exhibited a more negative charge following initial peptide association compared to unmodified CS, with the charge becoming less negative after electrostatically associated peptides were washed away (Figure 3c, Table 2). The lack of electrostatic interaction between CS and the associated peptide following the second high salt purification was confirmed using MALDI-TOF-MS (Supplemental Fig 1, Supplemental Fig 2) where following the initial purification, free peptide peaks were seen in the MALDI-TOF-MS; however, following the second purification, no free peptide was observed in the MALDI-TOF-MS spectrum.

Ultimately, the peptide GAG function is reliant on collagen binding; thus, the importance of the SRR spacer on the degree of peptide-GAG binding to collagen was analyzed. When applied to a collagen type I coated plate, the EC50 of the SRR-hyd conjugated peptide-GAG was an order of magnitude lower than the GSG-hyd conjugated peptide-GAG (Figure 3d). In addition, the SRR-hyd conjugated peptide-GAG EC50 was an order of magnitude lower than that of the former collagen-binding GAG synthesized using oxidation chemistry (Scott et al., 2013). There are several possible reasons for this difference in binding capacity. First, the SRR spacer sequence may be responsible for supporting covalent conjugation through the hydrazide (rather than amines present on the peptide) thereby orienting the peptide more favorably for collagen binding. Alternatively, the increase peptide conjugation efficiency, or number of peptides per GAG, could be contributing to the increased binding. The GSG-hyd peptide-GAG had significantly fewer peptides covalently attached to the GAG backbone and weaker collagen-binding. Regardless, the SRR spacer supports higher peptide-GAG conjugation efficiency and increased collagen binding capability of the peptide-GAG molecules.

3.2: Effect of C-terminal hydrazide on GQLY Conjugation and Collagen Binding Activity

Although the ECD chemistry was optimized to support hydrazide reactions with the carbonyl as opposed to amine reactions, it was possible that the internal lysine residues (ε-amine) and an N-terminal amines present in the GQLY peptides that could contribute to covalent bonds between the peptide and GAG. Thus, we tried to understand whether conjugation through the C-terminal hydrazide improved collagen binding. To explore this, a GQLY variant with the SRR spacer but with a non-reactive C-terminal amide, GQLYKSILYGSGSGSRR-amide (SRR-amide) was compared to the SRR-hyd peptide.

Following reaction with EDC, there was more SRR-hyd associated with CS compared to the SRR-amide variant (Figure 4a) suggesting that the SRR-hyd increase covalent conjugation, presumably through the more favorable hydrazide-COOH conjugation. In the absence of EDC, the amount of SRR-hyd and SRR-amide that associated with CS was equivalent

(Figure 4a). To determine if the difference in association following reaction in the presence of EDC was due to increased covalent conjugation, both peptide-GAG variants were washed with the concentrated salt and urea solution to remove the unbound peptides. Following this purification, both peptide-GAG variants exhibited similar decreases in associated peptides, with the SRR-hyd decreasing 5.2% and the SRR-amide peptide-GAG decreasing 5.7% in the associated peptide to GAG disaccharide ratio suggesting similar levels of peptide-GAG associate driven by electrostatic interactions (Figure 4b, Table 3). Furthermore, the level of associate peptide was significantly higher for the SRR-hyd variant than for than the SRR-amide variant following salt dissociation (Figure 3b), indicating that adding the C-terminal hydrazide supported increased covalent conjugation over that supported by the N-terminal amine and lysine. Zeta potential measurements of the molecules again confirmed this trend, with the molecules exhibiting an increased negative charge upon initial association with the GQLY variants and this charge becoming more positive after salt washing and dissociation (Figure 4c, Table 3).

Finally, to gain some insight as to whether N-terminal peptide conjugation vs. conjugation through the ε-amine of the lysine residues confers improved collagen binding, the collagen binding activity of the SRR-hyd and SRR-amide conjugated GAGs was determined. In this case, the EC50 of the SRR-hyd peptide-GAG was again a magnitude lower than that of the SRR-amide peptide-GAG (Figure 3c). Although there were still fewer peptides covalently bound to the GAG in the case of the SRR-amide variant, the magnitude of the difference between the two was less than the between the SRR-hyd and GSG-hyd variants. As such, while this difference in binding capacity may be explained by a difference in conjugated peptides, it also plausible, and indeed likely, that the conjugation through the hydrazide over the amines present in the collagen binding sequence of GQLY provides an improved presentation of the peptide to the collagen substrate. Taking the findings from the SRR-amide variant and the GSG-hyd variant together, it appears that having both the SRR spacer sequence and the C-terminal hydrazide are important to the collagen binding capacity of GQLY when conjugated to a GAG backbone.

3.3: Effect of GAG choice on GQLY Conjugation and Collagen Binding Activity

With the new understanding regarding how the SRR spacer and the C-terminal hydrazide affected conjugation to CS, we then sought to determine how the choice of GAG backbone affected the GQLY conjugation. For this, we looked at SRR-hyd conjugation to four GAG, heparin, CS, DS, and HA. Using these four GAGs allowed us to investigate SRR-hyd conjugation at three different GAG sulfation levels, with heparin being the most sulfated, HA being unsulfated, and CS and DS having similar, intermediate levels of sulfation. Following salt washing, the conjugation of GQLY to the GAG backbones correlated with this sulfation trend: heparin supported the greatest GQLY conjugation, HA supported the least, and CS and DS supported the same intermediate level of GQLY conjugation (Figure 5a). Similar to how the change in positive charge of the peptide affected how it interacted with the GAG backbone, the sulfation, and by extension the negative charge of the GAG, affected the level of GAG-peptide association.

Next, the effect of the GAG backbone on the collagen-binding ability of the peptide-GAGs was investigated using both heparin and CS. For this study, HA was not tested due to the significantly lower number of peptides attached. The investigation of the GAG-conjugates was examined before and after the salt wash to investigate whether electrostatically associated peptide contributed to glycoconjugate binding to collagen. Heparin and CS peptide-GAG binding to collagen was equivalent, with the EC50 of both being statistically similar to one another (Figure 5b). Furthermore, there was no difference in EC50 before and after the salt and urea washes (Figure 5b). This suggests that only covalently bound peptides contributed to the collagen binding of the peptide-GAG. Further, because electrostatically interacting peptide and peptide conjugated through ε-amine likely lie with the peptide backbone aligned more or less parallel to the GAG backbone rather than extending from the glycan backbone, while the peptide conjugated through the C-terminal hydrazide is more likely to extend from the backbone, this collagen-binding data suggests that peptide conjugated through the hydrazide shows a greater contribution to collagen binding than does peptide associated electrostatically or conjugated through the internal lysine residues of the peptide.

There has been an increase in the use of conjugated peptides for biomedical uses over the past several decades (Akkiraju et al., 2017; Deloney et al., 2021; Hao et al., 2023; Park et al., 2019; Yao et al., 2016). Compared to proteins, peptides are significantly simpler and cheaper to produce yet provide an intended biological function (Hosoyama et al., 2019). However, many peptides used still require custom synthesis, adding to their cost and the complexity of the synthesis of the final product (Collier & Segura, 2011). As such, maximizing the reaction efficiency between the peptide and the substrate can improve the clinical translatability of peptide conjugated molecules and materials through reducing the peptide required to achieve desired conjugation targets. From this work, we have demonstrated that relatively simple changes to the non-functional portions of the peptide, the peptide spacer sequence, can have significant effects on the conjugation efficiency of a positively charged peptide to a negatively charged GAG. Conversely, the charge properties of the GAG also effected the peptide/GAG conjugation efficiency. As such, modulating the charge between the peptide and the conjunction substrate can be a method to increase the efficiency of conjugation.

3.4 Platelet-collagen inhibition

To evaluate the preserved biological activity of the GAG component of the bioconjugate, the ability of HEP-GQLY-SRR (amide and hydrazide variants) to inhibit platelet binding to collagen was investigated. While both Hep-GQLY-SRR and CS-GQLY-SRR showed maximal peptide conjugation and collagen binding, heparin is known to suppress platelet binding (Biran & Pond, 2017; Linhardt et al., 2008). Thus, platelet inhibition and in vivo studies were limited to hep-GQLY-SRR. Strong inhibition of platelet adhesion to immobilized fibrillar collagen was observed with hep-GQLY-SRR in a dose-dependent manner resulting in an IC50 of about 59 ug/mL (or approximately 3 uM). Maximal platelet inhibition was observed at about 0.5 mg/mL, at which more than 90% inhibition was achieved relative to untreated control channels (Figure 6a, Figure S5). While this does translate to a higher concentration of heparin compared to the effective hourly dosages for

preventing platelet adherence in preclinical studies, the GAG-conjugate molecule would only need to be delivered as a single treatment due to it localizing to the site of injury (Hoover et al., 1980). As such, continuous infusion of heparin would not be required, reducing the total heparin delivered to the body and alleviating the concern of systemic anti-platelet activity. Furthermore, the components of Hep-GQLY alone, unmodified heparin and free GQLY peptide, demonstrated no significant platelet inhibition, even at high concentrations (Figure 6b). This implies the necessity of both the collagen-binding ability of GQLY and the bioactive properties of heparin in a combined molecule for effective platelet inhibition under flow.

3.5 In vivo targeted delivery

Targeted delivery to areas of vessel injury was evaluated in a rabbit artery crush model with intravenous injection of fluorescently labeled Hep-GQLY-SRR at varying concentrations. Given the lack of platelet inhibition by the individual components of Hep-GQLY (Hep or GQLY only) in *in vitro* conditions, only the Hep-GQLY molecule was tested in vivo at varying doses. The appearance of fluorescence in regions of arterial clamp injuries was observed weakly at 0.16 mg/kg and with a strong signal at 1.6 mg/kg. No signal was observed in the vehicle control group or at 0.016 mg/kg dose level. Representative images from the various Hep-GQLY-SRR concentrations are shown in Figure 7. Importantly, no fluorescence signal was observed in areas of the vessel was that were not subject to clamp injury, indicating that targeted delivery only to areas of injury was achieved.

Collagen-targeting biomolecules have a myriad of potential diagnostic and therapeutic uses given collagen’s ubiquity throughout the body(Wahyudi et al., 2016). Several collagen binding peptides have been developed from native sources including the platelet collagen binding receptor(Stuart et al., 2011) and the leucine rich repeat units of decorin(Federico et al., 2015; Hunter et al., 2001). In this study, we employed a modified version of a previously used platelet derived collagen binding sequence, RRANAALKAGELYKSILYGC, with the benefit of the GQLY sequence being its shorter sequence, resulting in a simpler and quicker synthesis(Stuart et al., 2011). Furthermore, by using a C-terminal hydrazide we no longer relied on oxidation of the GAG rings(Stuart et al., 2011) or a heterobifunctional crosslinker(Scott et al., 2013) to conjugate the peptide to the GAG backbone, maintaining the GAG structure and simplifying the chemistry. Although it is possible for conjugation to occur through amines present on the peptide, we have demonstrated that the presence of the C-terminal hydrazide potentially drives greater conjugation through the hydrazide as opposed to the primary amines, improving the collagen binding ability of the molecule.

Additionally, through the addition of cationic charge to the spacer sequence of our collagen binding peptide, we were able to increase the binding capability of our peptide-GAG conjugate molecules. With minimal modification to the binding sequence, changes to the peptide spacer sequence resulted in a significant increase in collagen binding activity. This increased binding capability may allow for increased residence time within the body, prolonging the therapeutic life of the molecule. Alternatively, increased binding capability of the peptide can allow for a reduced number of peptides required for effective binding, resulting in reduced modification of the GAG backbone for increased GAG

bioactivity(Nguyen et al., 2021) or increases in the number of additional therapeutic peptides(Walimbe et al., 2021). Altogether, modulation of the peptide spacer sequence can allow for simplification of the conjugation chemistry, increased conjugation yields, and improved biological activity without the need for modification of the core peptide sequence.

Conclusions:

Data obtained through this study demonstrated that the peptide spacer is important to efficient peptide conjugation to GAG. The use of cationic charge proximal to the hydrazide group can improve peptide GAG interaction, which increases conjugation through the hydrazide functional group. Further, C-terminal conjugation appears to be critical in increasing the interaction of the peptide-GAG conjugate with collagen. This work suggests that including cationic charge in the intended bioconjugate can be used to increase the conjugation efficiency of peptides and other chemicals to GAGs.

Supplementary Material

Refer to Web version on PubMed Central for supplementary material.

Acknowledgements:

This work was funded in part by the NIH grant T32 HL086350

Abbreviations:

Hep	heparin
DS	dermatan sulfate
CS	chondroitin sulfate
HA	hyaluronic acid
SRR-hyd	GQLYKSILYGSGSGSRR-hydrazide
SRR-amide	GQLYKSILYGSGSGSRR-amide
GSG-hyd	GQLYKSILYGSGSG-hydrazide
FPLC	fast protein liquid chromatography
MALDI-TOF MS	matrix assisted laser desorption/ionization time of flight mass spectrometry
MES	2-(N-morpholino)ethanesulfonic acid
EDC	1-ethyl-3-[3-dimethylaminopropyl]carbodiimide
PBS	phosphate buffered saline
DMSO	dimethylsulfoxide

References:

Akkiraju H, Srinivasan PP, Xu X, Jia X, Safran CBK, & Nohe A (2017). CK2.1, a bone morphogenetic protein receptor type Ia mimetic peptide, repairs cartilage in mice with destabilized medial meniscus. Stem Cell Research & Therapy, 8(1), 82. 10.1186/s13287-017-0537-y [PubMed: 28420447]

Biran R, & Pond D (2017). Heparin coatings for improving blood compatibility of medical devices. Advanced Drug Delivery Reviews, 112, 12–23. 10.1016/j.addr.2016.12.002 [PubMed: 28042080]

Capila I, & Linhardt RJ (2002). Heparin–Protein Interactions. Angewandte Chemie International Edition, 41(3), 390–412. 10.1002/1521-3773(20020201)41:3<390::AID-ANIE390>3.0.CO;2-B

Chiang TM, & Kang AH (1997). A synthetic peptide derived from the sequence of a type I collagen receptor inhibits type I collagen-mediated platelet aggregation. The Journal of Clinical Investigation, 100(8), 2079–2084. 10.1172/JCI119741 [PubMed: 9329973]

Cho Y-S, & Han Ahn K (2013). Molecular interactions between charged macromolecules: Colorimetric detection and quantification of heparin with a polydiacetylene liposome. Journal of Materials Chemistry B, 1(8), 1182–1189. 10.1039/C2TB00410K [PubMed: 32260841]

Collier JH, & Segura T (2011). Evolving the use of peptides as biomaterials components. Biomaterials, 32(18), 4198–4204. 10.1016/j.biomaterials.2011.02.030 [PubMed: 21515167]

D'Agnillo F, Walters K-A, Xiao Y, Sheng Z-M, Scherler K, Park J, Gygli S, Rosas LA, Sadtler K, Kalish H, Blatti CA, Zhu R, Gatzke L, Bushell C, Memoli MJ, O'Day SJ, Fischer TD, Hammond TC, Lee RC, … Taubenberger JK (2021). Lung epithelial and endothelial damage, loss of tissue repair, inhibition of fibrinolysis, and cellular senescence in fatal COVID-19. Science Translational Medicine, 13(620), eabj7790. 10.1126/scitranslmed.abj7790 [PubMed: 34648357]

Das Kurmi B, Tekchandani P, Paliwal R, & Rai Paliwal S (2015). Nanocarriers in Improved Heparin Delivery: Recent Updates. Current Pharmaceutical Design, 21(30), 4509–4518. [PubMed: 26295952]

Deloney M, Garoosi P, Dartora VFC, Christiansen BA, & Panitch A (2021). Hyaluronic Acid-Binding, Anionic, Nanoparticles Inhibit ECM Degradation and Restore Compressive Stiffness in Aggrecan-Depleted Articular Cartilage Explants. Pharmaceutics, 13(9), Article 9. 10.3390/pharmaceutics13091503

Federico S, Pierce BF, Piluso S, Wischke C, Lendlein A, & Neffe AT (2015). Design of Decorin-Based Peptides That Bind to Collagen I and their Potential as Adhesion Moieties in Biomaterials. Angewandte Chemie International Edition, 54(37), 10980–10984. 10.1002/anie.201505227 [PubMed: 26216251]

Han HD, Lee A, Song CK, Hwang T, Seong H, Lee CO, & Shin BC (2006). In vivo distribution and antitumor activity of heparin-stabilized doxorubicin-loaded liposomes. International Journal of Pharmaceutics, 313(1), 181–188. 10.1016/j.ijpharm.2006.02.007 [PubMed: 16540270]

Hao D, Liu R, Fernandez TG, Pivetti C, Jackson JE, Kulubya ES, Jiang H-J, Ju H-Y, Liu W-L, Panitch A, Lam KS, Leach JK, Farmer DL, & Wang A (2023). A bioactive material with dual integrin-targeting ligands regulates specific endogenous cell adhesion and promotes vascularized bone regeneration in adult and fetal bone defects. Bioactive Materials, 20, 179–193. 10.1016/j.bioactmat.2022.05.027 [PubMed: 35663336]

Harifi G, & Sibilia J (2016). Pathogenic role of platelets in rheumatoid arthritis and systemic autoimmune diseases. Saudi Medical Journal, 37(4), 354–360. 10.15537/smj.2016.4.14768 [PubMed: 27052277]

Hoover RL, Rosenberg R, Haering W, & Karnovsky MJ (1980). Inhibition of rat arterial smooth muscle cell proliferation by heparin. II. In vitro studies. Circulation Research, 47(4), 578–583. 10.1161/01.res.47.4.578 [PubMed: 6157501]

Hosoyama K, Lazurko C, Muñoz M, McTiernan CD, & Alarcon EI (2019). Peptide-Based Functional Biomaterials for Soft-Tissue Repair. Frontiers in Bioengineering and Biotechnology, 7. https://www.frontiersin.org/articles/10.3389/fbioe.2019.00205

Hunter GK, Poitras MS, Underhill TM, Grynpas MD, & Goldberg HA (2001). Induction of collagen mineralization by a bone sialoprotein–decorin chimeric protein. Journal of Biomedical Materials

Research, 55(4), 496–502. 10.1002/1097-4636(20010615)55:4<496::AID-JBM1042>3.0.CO;2-2 [PubMed: 11288077]

Karsdal MA, Nielsen SH, Leeming DJ, Langholm LL, Nielsen MJ, Manon-Jensen T, Siebuhr A, Gudmann NS, Rønnow S, Sand JM, Daniels SJ, Mortensen JH, & Schuppan D (2017). The good and the bad collagens of fibrosis – Their role in signaling and organ function. Advanced Drug Delivery Reviews, 121, 43–56. 10.1016/j.addr.2017.07.014 [PubMed: 28736303]

Liang Y, & Kiick KL (2014). Heparin-functionalized polymeric biomaterials in tissue engineering and drug delivery applications. Acta Biomaterialia, 10(4), 1588–1600. 10.1016/j.actbio.2013.07.031 [PubMed: 23911941]

Linhardt RJ, Murugesan S, & Xie J (2008). Immobilization of Heparin: Approaches and Applications. Current Topics in Medicinal Chemistry, 8(2), 80–100. 10.2174/156802608783378891 [PubMed: 18289079]

Malloy RJ, Rimsans J, Rhoten M, Sylvester K, & Fanikos J (2018). Unfractionated Heparin and Low-Molecular-Weight Heparin. In Lau JF, Barnes GD, & Streiff MB (Eds.), Anticoagulation Therapy (pp. 31–57). Springer International Publishing. 10.1007/978-3-319-73709-6_3

Manon-Jensen T, Kjeld NG, & Karsdal MA (2016). Collagen-mediated hemostasis. Journal of Thrombosis and Haemostasis, 14(3), 438–448. 10.1111/jth.13249 [PubMed: 26749406]

Micsonai A, Wien F, Bulyáki É, Kun J, Moussong É, Lee Y-H, Goto Y, Réfrégiers M, & Kardos J (2018). BeStSel: A web server for accurate protein secondary structure prediction and fold recognition from the circular dichroism spectra. Nucleic Acids Research, 46(W1), W315–W322. 10.1093/nar/gky497 [PubMed: 29893907]

Micsonai A, Wien F, Kernya L, Lee Y-H, Goto Y, Réfrégiers M, & Kardos J (2015). Accurate secondary structure prediction and fold recognition for circular dichroism spectroscopy. Proceedings of the National Academy of Sciences, 112(24), E3095–E3103. 10.1073/pnas.1500851112

Naggi A, Casu B, Perez M, Torri G, Cassinelli G, Penco S, Pisano C, Giannini G, Ishai-Michaeli R, & Vlodavsky I (2005). Modulation of the heparanase-inhibiting activity of heparin through selective desulfation, graded N-acetylation, and glycol splitting. The Journal of Biological Chemistry, 280(13), 12103–12113. 10.1074/jbc.M414217200 [PubMed: 15647251]

Nguyen M, Liu JC, & Panitch A (2021). Physical and Bioactive Properties of Glycosaminoglycan Hydrogels Modulated by Polymer Design Parameters and Polymer Ratio. Biomacromolecules. 10.1021/acs.biomac.1c00866

Nording HM, Seizer P, & Langer HF (2015). Platelets in Inflammation and Atherogenesis. Frontiers in Immunology, 6. https://www.frontiersin.org/articles/10.3389/fimmu.2015.00098

Paderi JE, Stuart K, Sturek M, Park K, & Panitch A (2011). The inhibition of platelet adhesion and activation on collagen during balloon angioplasty by collagen-binding peptidoglycans. Biomaterials, 32(10), 2516–2523. 10.1016/j.biomaterials.2010.12.025 [PubMed: 21216002]

Paderi J, Prestwich GD, Panitch A, Boone T, & Stuart K (2018). Glycan Therapeutics: Resurrecting an Almost Pharma-Forgotten Drug Class. Advanced Therapeutics, 1(8), 1800082. 10.1002/adtp.201800082

Park SH, Seo JY, Park JY, Ji YB, Kim K, Choi HS, Choi S, Kim JH, Min BH, & Kim MS (2019). An injectable, click-crosslinked, cytomodulin-modified hyaluronic acid hydrogel for cartilage tissue engineering. NPG Asia Materials, 11(1), 1–16. 10.1038/s41427-019-0130-1

Schick BP, Maslow D, Moshinski A, & Antonio JDS (2004). Novel concatameric heparin-binding peptides reverse heparin and low-molecular-weight heparin anticoagulant activities in patient plasma in vitro and in rats in vivo. Blood, 103(4), 1356–1363. 10.1182/blood-2003-07-2334 [PubMed: 14576044]

Scott RA, Paderi JE, Sturek M, & Panitch A (2013). Decorin Mimic Inhibits Vascular Smooth Muscle Proliferation and Migration. PLOS ONE, 8(11), e82456. 10.1371/journal.pone.0082456 [PubMed: 24278482]

Strobel HA, Qendro EI, Alsberg E, & Rolle MW (2018). Targeted Delivery of Bioactive Molecules for Vascular Intervention and Tissue Engineering. Frontiers in Pharmacology, 9. https://www.frontiersin.org/articles/10.3389/fphar.2018.01329

Stuart K, Paderi J, Snyder PW, Freeman L, & Panitch A (2011). Collagen-Binding Peptidoglycans Inhibit MMP Mediated Collagen Degradation and Reduce Dermal Scarring. PLOS ONE, 6(7), e22139. 10.1371/journal.pone.0022139 [PubMed: 21779387]

Vallet SD, Clerc O, & Ricard-Blum S (2021). Glycosaminoglycan–Protein Interactions: The First Draft of the Glycosaminoglycan Interactome. Journal of Histochemistry & Cytochemistry, 69(2), 93–104. 10.1369/0022155420946403 [PubMed: 32757871]

Wahyudi H, Reynolds AA, Li Y, Owen SC, & Yu SM (2016). Targeting collagen for diagnostic imaging and therapeutic delivery. Journal of Controlled Release, 240, 323–331. 10.1016/j.jconrel.2016.01.007 [PubMed: 26773768]

Walimbe T, Dehghani T, Casella A, Lin J, Wang A, & Panitch A (2021). Proangiogenic Collagen-Binding Glycan Therapeutic Promotes Endothelial Cell Angiogenesis. ACS Biomaterials Science & Engineering, 7(7), 3281–3292. 10.1021/acsbiomaterials.1c00336 [PubMed: 34192455]

Wang P, Chi L, Zhang Z, Zhao H, Zhang F, & Linhardt RJ (2022). Heparin: An old drug for new clinical applications. Carbohydrate Polymers, 295, 119818. 10.1016/j.carbpol.2022.119818 [PubMed: 35989029]

Yao Y, Zeng L, & Huang Y (2016). The enhancement of chondrogenesis of ATDC5 cells in RGD-immobilized microcavitary alginate hydrogels. Journal of Biomaterials Applications, 31(1), 92–101. 10.1177/0885328216640397 [PubMed: 27000189]

Yu D, Makkar G, Sarkar R, Strickland DK, & Monahan TS (2017). Murine Aortic Crush Injury: An Efficient In Vivo Model of Smooth Muscle Cell Proliferation and Endothelial Function. Journal of Visualized Experiments: JoVE, 124, 55201. 10.3791/55201

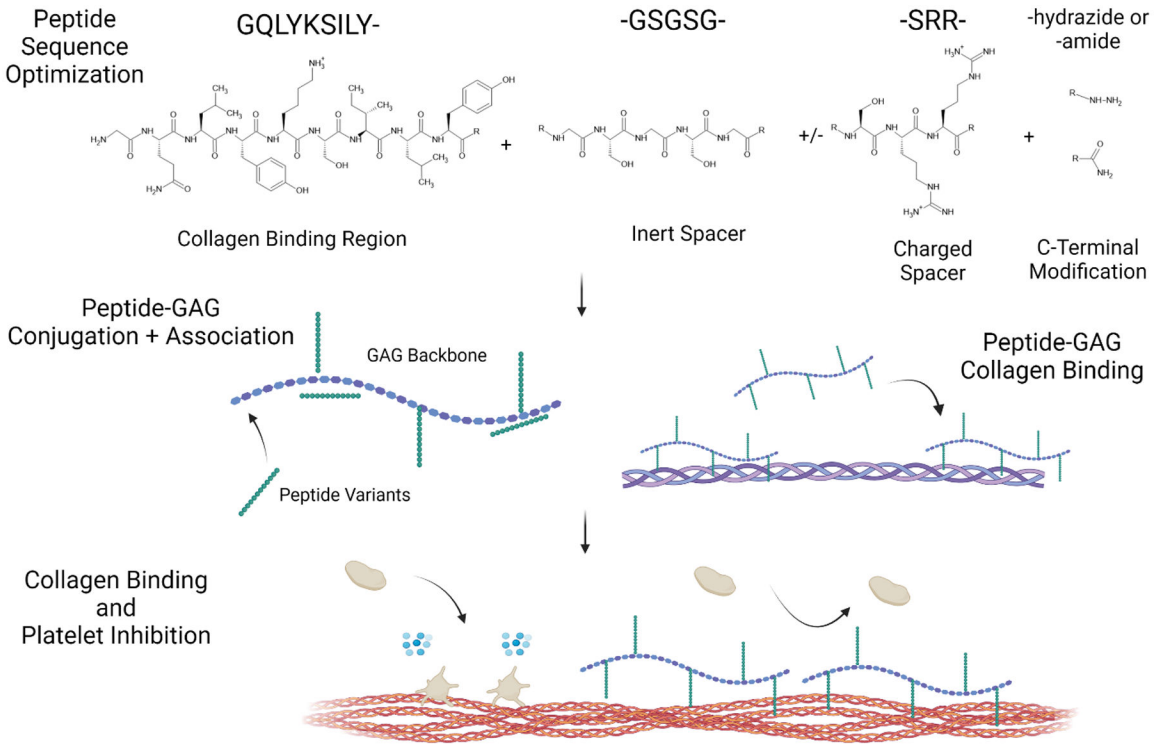

Figure 1:
Experiment scheme for GQLY sequence optimization. GAG, Glycosaminoglycan (Created with Biorender.com)

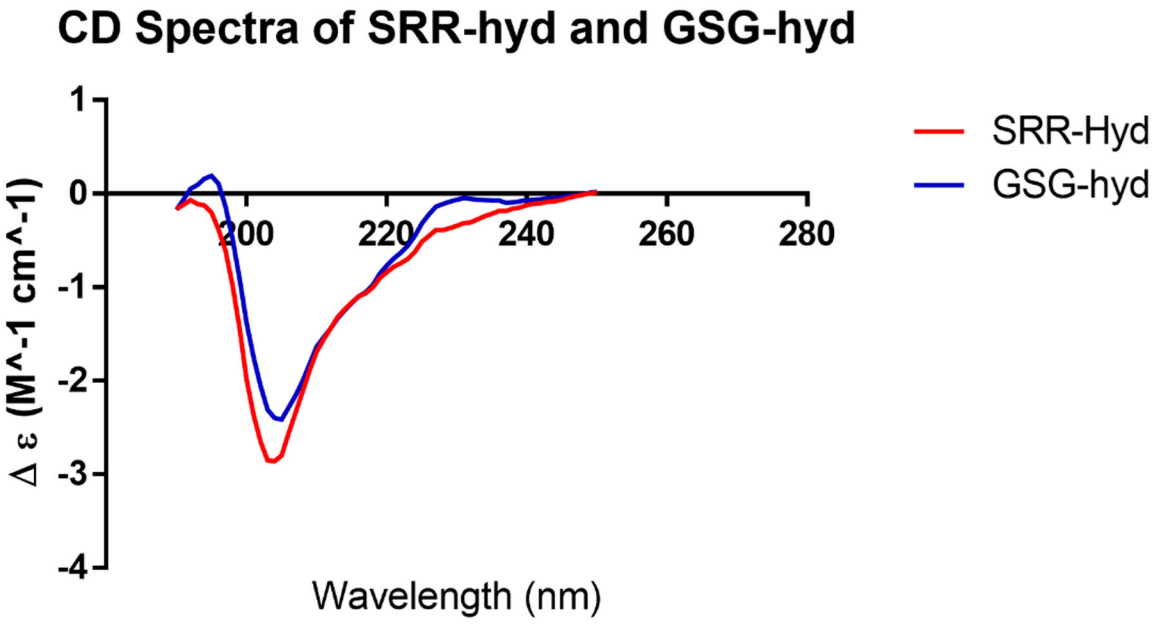

Figure 2:

CD Spectra of SRR-hyd and GSG-hyd GQLY variant peptides. Data was baseline corrected and matched concentrations (1 mg/ml) were used. Data was then analyzed using BESTSEL (https://bestsel.elte.hu/index.php).

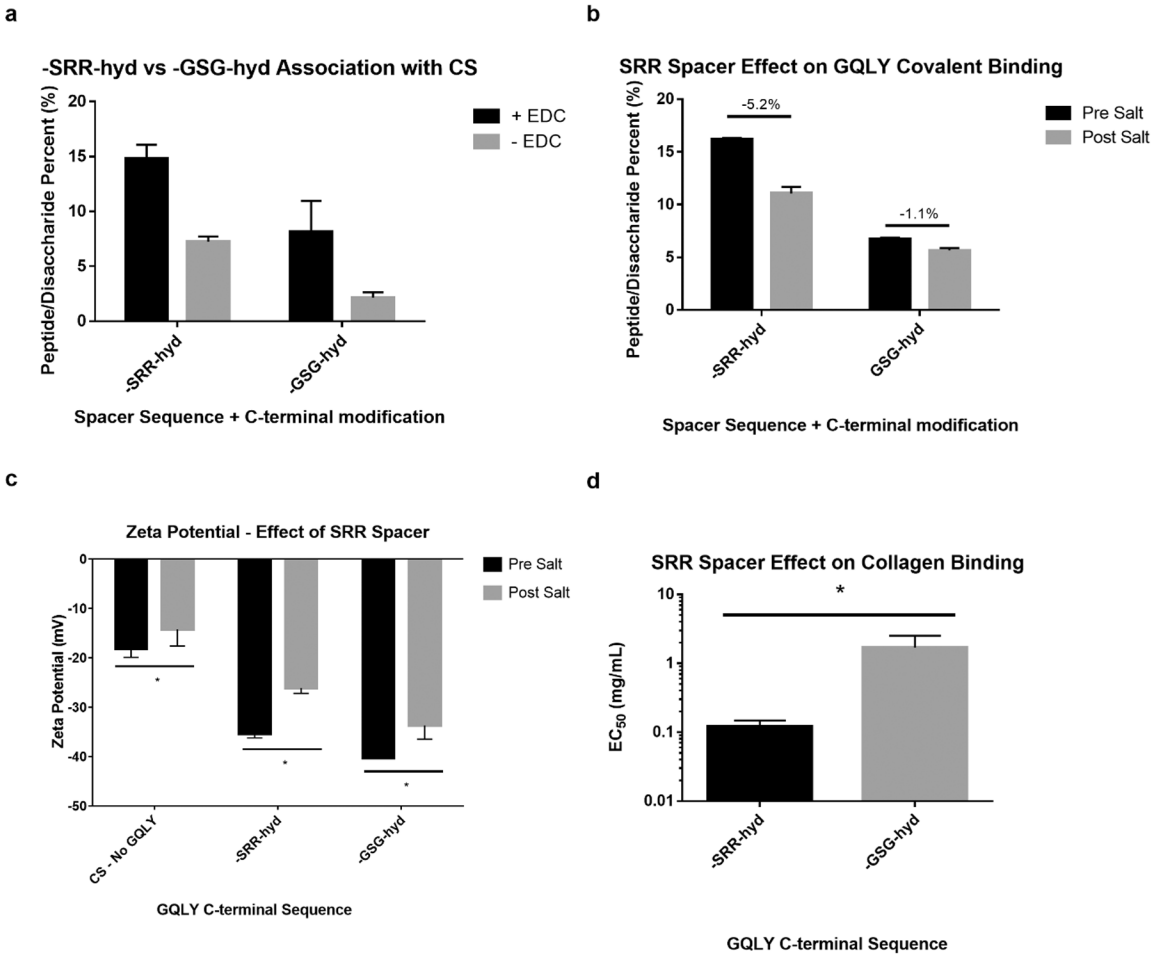

Figure 3:

Effect of SRR spacer on peptide-GAG association and collagen binding. A) Associated SRR-hyd or GSG-hyd with CS with and without EDC. B) Associated peptide before and after 1M NaCl and 8M Urea wash and filtration. C) Zeta potential of CS only, CS with SRR-hyd, and CS with GSG-hyd before and after 1M NaCl and 8M Urea wash and filtration. D) EC_{50} (EC_{50} concentration of collagen at which fluorescent signal CS-GQLY was 50% of maximum signal) of CS-GQLY on collagen type I surface with either SRR-hyd or GSG-hyd. * denotes statistical significance ($P < 0.05$) between groups.

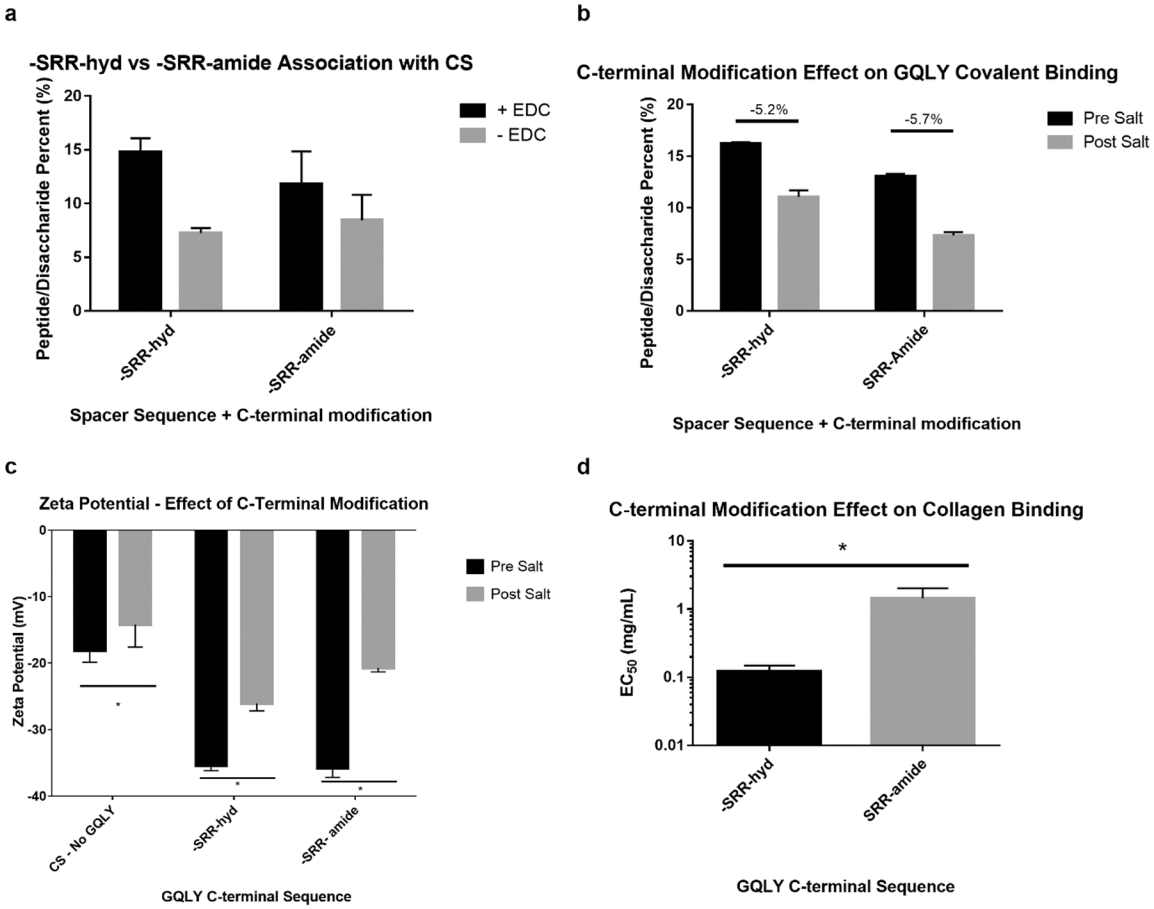

Figure 4:

Effect of C-terminal modification of GQLY on peptide-GAG association and collagen binding. A) Associated SRR-hyd or SRR-amide with CS with and without EDC. B) Associated peptide before and after 1M NaCl and 8M Urea wash and filtration. C) Zeta potential of CS only, CS with SRR-hyd, and CS with SRR-amide before and after 1M NaCl and 8M Urea wash and filtration. D) EC50 of CS-GQLY on collagen type I surface with either SRR-hyd or SRR-amide. * denotes statistical significance ($P < 0.05$) between groups. n.s. denotes no statistical significance between groups

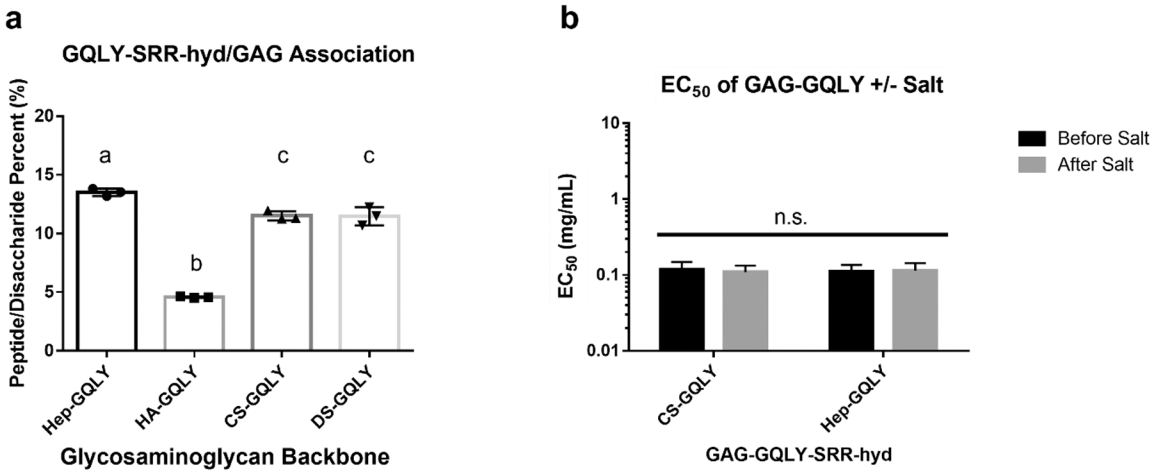

Figure 5:

Effect of GAG backbone on peptide-GAG association and collagen binding. A) SRR-hyd conjugation with heparin, HA, CS, and DS. B) EC50 of CS-GQLY and Hep-GQLY on collagen type I. Groups that do not share a letter are statistically significant ($P < 0.05$) from one other. N.s. denotes no statistical significance between groups.

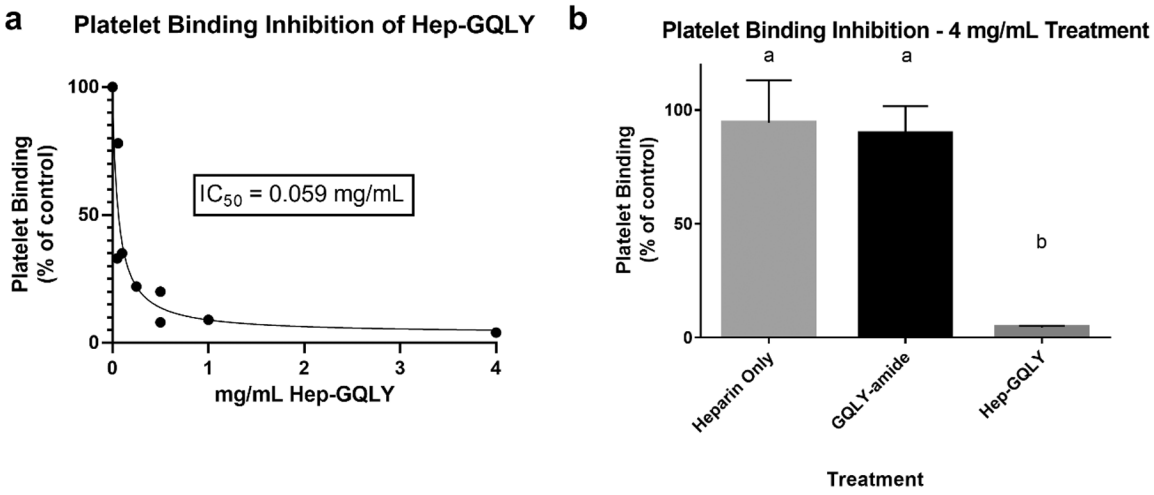

Figure 6:

Platelet Inhibition by Hep-GQLY. A) IC50 determination of Hep-GQLY platelet inhibition. B) Platelet inhibition by unmodified heparin, GQLY peptide, and Hep-GQLY. Groups that do not share a letter are statistically significant

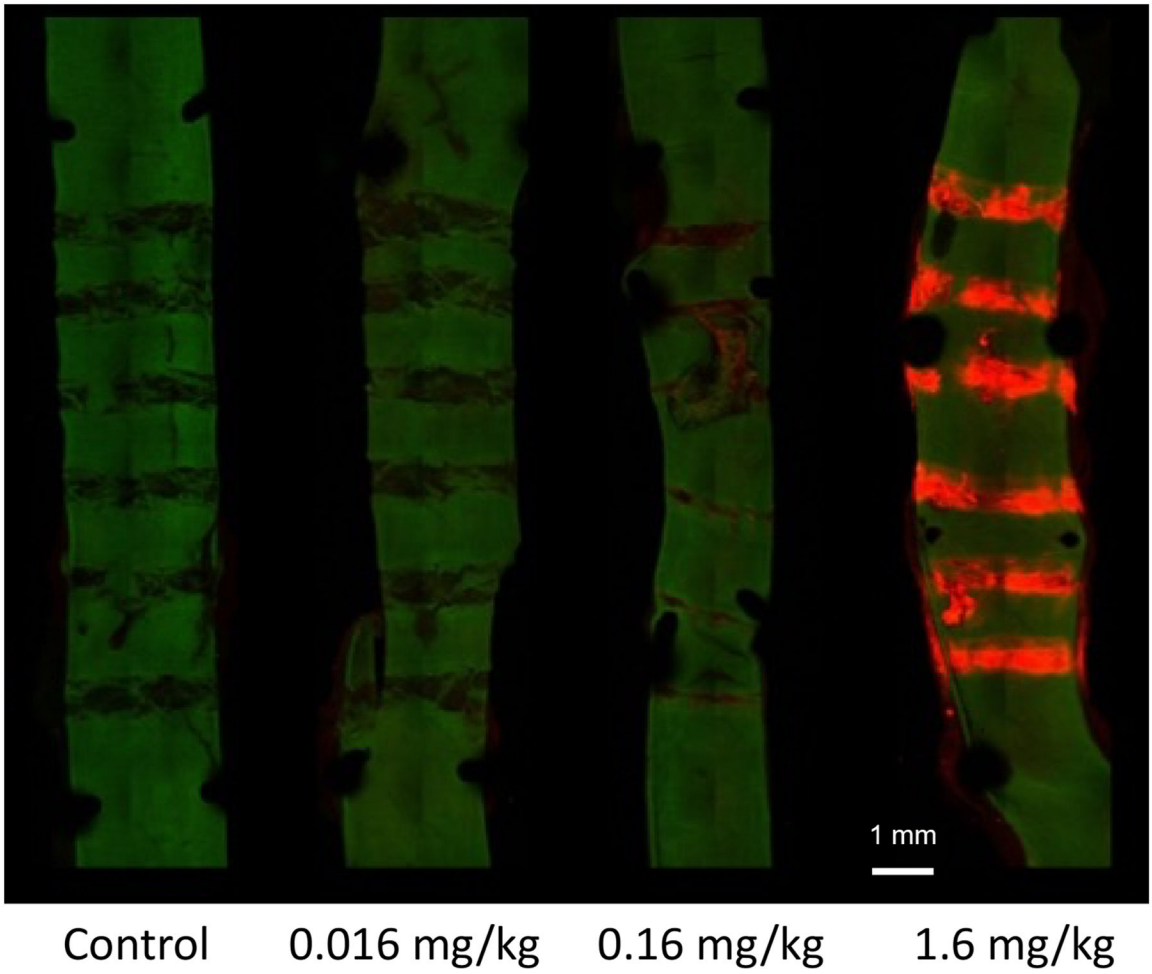

Figure 7:
Fluorescently labeled Hep-GQLY-SRR localization to site of carotid artery crush. Maximum intensity projection with tissue autofluorescence shown in green, and fluorescently conjugated molecule shown in red localizing to areas of crush injury.

Table 1:

Secondary structure calculations of GQLY variants SRR-hyd and GSG-hyd

	Helix	Antiparallel	Parallel	Turn	Others
SRR-hyd	5.5	21.8	0	13.5	59.2
GSG-hyd	6.2	25.6	0	14.3	53.9

Table 2:

Change in peptide-GAG association before and after salt and urea wash

	Pre-Salt Peptide/ Disaccharide Ratio	Pre-Salt Zeta Potential	Post-Salt Peptide/ Disaccharide Ratio	Post-Salt Zeta Potential	Percent Decrease in total peptide associated/GAG
CS + SRR-hyd	16.3%	−35.4 mV	11.1%	−26.1 mV	32%
CS + GSG-hyd	6.7%	−40.3 mV	5.6%	−33.7 mV	15%

Table 3:

Change in SRR-hyd and SRR-amide association before and after salt and urea wash

	Pre-Salt Peptide/ Disaccharide Ratio	Pre-Salt Zeta Potential	Post-Salt Peptide/ Disaccharide Ratio	Post-Salt Zeta Potential	Percent Decrease in total peptide associated/GAG
CS + SRR-hyd	16.3%	−35.4 mV	11.1%	−26.1 mV	32%
CS + SRR-amide	13.1%	−35.8 mV	7.4%	−20.7 mV	44%